Available online at www.sciencedirect.com
ScienceDirect
Transportation Research Procedia 7 (2015) 381 – 397
Transportation Research Procedia
www.elsevier.com/locate/procedia

21st International Symposium on Transportation and Traffic Theory, ISTTT21 2015, 5-7 August 2015, Kobe, Japan

Continuum Theory for Pedestrian Traffic Flow: Local Route Choice Modelling and its Implications

Serge P. Hoogendoorn [a,*], Femke van Wageningen-Kessels [a], Winnie Daamen [a], Dorine C. Duives [a], Majid Sarvi [b]

[a] *Transport & Planning, Delft University of Technology, Stevinweg 1, 2628 CN, Delft, The Netherlands*
[b] *Monash University, Australia*

Abstract

This contribution puts forward a novel multi-class continuum model that captures some of the key dynamic features of pedestrian flows. It considers route choice behaviour on both the strategic (pre-trip) and tactical (en-route) level. To achieve this, we put forward a class-specific equilibrium direction relation of the pedestrians, which is governed by two parts: one part describing the global route choice, which is pre-determined based on the expectations of the pedestrians, and one part describing the local route choice, which is a density-gradient dependent term that reflects local adaptations based on prevailing flow conditions.

Including the local route choice term in the multi-class model causes first of all dispersion of the flow: pedestrians will move away from high density areas in order to reduce their overall walking costs. Second of all, for the crossing flow and bi-directional flow cases, local route choice causes well known self-organised patterns to emerge (i.e. diagonal stripes and bi-directional lanes). We study under which demand conditions self-organisation occurs and fails, as well as what the impact is of the choices of the different model parameters. In particular, the differences in the weights reflecting the impact of the own and the other classes appear to have a very strong impact on the self-organisation process.

Selection and peer-review under responsibility of Kobe University
Keywords: Continuum flow modelling; local route choice; hybrid modelling.

1. Introduction

Although microscopic pedestrian flow modelling has received quite some attention in the past decade, a comprehensive macroscopic theory for pedestrian traffic operations has not been put forward. Amongst the limited contributions are the papers of Hughes (2002) and Hoogendoorn and Bovy (2004a), both using a combination of a conservation of pedestrians equation and a global route choice model. Both papers propose iterative frameworks to achieve consistency between assigning pedestrians to the available space and the delays caused by overcrowding of some of the routes. However, for simulation purposes, these frameworks are impractical due to the lengthy computation times,

* Corresponding author. Tel.: +31-15-2785475.
E-mail address: s.p.hoogendoorn@tudelft.nl

Selection and peer-review under responsibility of Kobe University
doi:10.1016/j.trpro.2015.06.020

the poor convergence behaviour, and the unrealistic behavioural assumptions. Furthermore, to the best of our knowledge, none of the macroscopic models presented in literature captures the key features of pedestrian flows, such as the different types of self-organisation (e.g. dynamic lane formation); see Helbing et al. (2005).

This paper presents a new continuum pedestrian flow model that remedies some of the key issues observed in previous macroscopic flow models. This is achieved by including a local route choice next to global route choice. In the proposed model, local route choice in achieved by including a *local value or potential function*. This term causes an increase in flux into areas with a relatively low density, yielding a natural spatial distribution of the density. The local route choice model also provides a unique mechanism that enables reproduction of dynamic lane formation and other types flow separation (e.g. formation of diagonal stripes; see Helbing et al. (2005)).

The main contribution of the presented work is the new mathematical modelling framework for two-dimensional continuum pedestrian flow, which reproduces realistic (self-organised) pedestrian traffic operation features. Using efficient solves, the macroscopic model can be used to simulate large-scale areas, which is more difficult using microscopic models. Furthermore, macroscopic models such as the model presented here, can be used in optimisation frameworks, such as described in Hoogendoorn et al. (2013).

After the introduction and literature review in section 2, we present a generic first order pedestrian flow model in section 3. In section 4 we introduce the local route choice model and show how it generalises the model presented in Hoogendoorn et al. (2014). In section 5 we apply simulations to show that the model reproduces some important phenomena, such as lane and stripe formation, and we illustrate the influence of the model parameters on the simulation results. We conclude this contribution with conclusions in section 6.

2. State-of-the-art

In this section, we review some of the key studies that form the foundation of the model presented in this manuscript. While not trying to be complete, we briefly present relevant empirical studies, as well as the main modelling approaches that have been put forward, with an emphasis on continuum models. In particular the latter type of models will be discussed in more detail, focussing on their ability to reproduce the aforementioned pedestrian flow phenomena.

2.1. Empirical features

Previous empirical and experimental studies of pedestrian flow characteristics showed many interesting features, including the existence of a fundamental relation between density and flow and self-organised structures (Schadschneider et al. (2009)). As the combination of the fundamental diagram and different phenomena of self-organisation characterise pedestrian dynamics, begin fundamental for a macroscopic model, these are briefly discussed in this section.

The fundamental relation reflects the statistical relation between density ρ and (absolute) flow Q or speed V, i.e. $V = V(\rho)$ or $Q = \rho \cdot V = Q(\rho)$; see Weidmann (1993). Many factors influence the shape of this fundamental relation. Chattaraj et al. (2009) show the effect of cultural differences on the shape of the fundamental relation. The characteristic values of the fundamental diagram, such as the capacity and the jam density, are also influenced by factors such as trip purpose (Oeding (1963)) and the heterogeneity of the pedestrians (Helbing et al. (2007)). Its shape also varies for various types of facilities (such as stairs, ramps and bottlenecks) and the direction of the pedestrian flows (unidirectional or bi-directional) (Weidmann (1993); Navin and Wheeler (1969)).

Self-organisation is defined as the spontaneous occurrence of qualitatively new behaviour through the non-linear interaction of many objects or subjects (Helbing and Johansson (2010)) without the intervention of external influences (Camazine et al. (2010)).

The most common self-organisation phenomenon is lane formation (Hoogendoorn and Daamen (2004)). During this process a number of lanes of varying width form dynamically in a corridor. Next to lane formation in bi-directional flows, diagonal stripe formation in crossing flows has been observed; e.g. see Hoogendoorn and Daamen (2004).

During their research at the Jamarat bridge, Helbing et al. (2007) found stop & go waves. These are temporarily interrupted longitudinal flows that appear at higher densities in uni-directional crowds. In an even denser flow regime,

turbulent flows were found. In this regime a pedestrian has no control over its own movements anymore. Local force based interactions between pedestrian bodies are seen.

Three other effects have been described at an operational level, namely herding, the zipper effect and the faster-is-slower effect. Herding occurs when unclarity of the situation causes individuals to follow each other instead of taking the optimal route (Helbing et al. (2005)). This behaviour is predominantly seen during stressful evacuation situations. The zipper effect describes the situation in which individuals allow others within the territorial space diagonally in front of them, as long as the direct space in front of their feet is still empty (Hoogendoorn and Daamen (2005)). It allows for narrower lanes in a bottleneck than expected based on the width of a pedestrians territorial zone. The faster-is-slower effect describes a situation where the density in a queue upstream of a bottleneck is increasing, due to the fact that people keep heading forward while the bottleneck is clogged (Helbing and Johansson (2010)). The higher densities cause coordination problems since a large number of individuals is competing for a few small gaps. Bodily interaction and friction slow down the total crowd motion.

2.2. Modelling approaches

Pedestrian flow literature often distinguishes microscopic and macroscopic models. *Microscopic models* represent pedestrian flow at the level of individual pedestrians, and generally aim to describe the individual behaviour and interactions. On the contrary, *macroscopic models* describe the flow dynamics in more aggregate terms, using quantities such as flows, densities, and speeds.

Duives et al. (2013) compared a number of pedestrian flow modelling approaches, focussing on how well these models are able to simulate the key phenomena indicated in the previous paragraphs. The paper discusses different types of models, such as cellular automata, social force models, velocity-based models, continuum models, hybrid models, behavioral models and network models. The comparison shows that "the models can roughly be divided into slow but highly precise microscopic modelling attempts and very fast but behaviourally questionable macroscopic modelling attempts".

2.2.1. Microscopic and mesoscopic walker models

In the last few decades several streams of microscopic and mesoscopic walker models have been developed. The first stream of microscopic models were *Cellular Automata* (Blue and Adler (1998); Blue and Adler (2001)), which describe the movement of agents through a simulated environment using a discrete representation of both space and time.

A second stream of microscopic models, *Social Force models*, was introduced by Helbing and Molnar (1995). These models simulate movements based on deterministic force-based interactions and have a continuous representation of space. The effects modelled might be physical in appearance (collisions) or used to model interaction with elements or humans within the movement space (human interaction, light effects, attraction zones, etc.). Numerous adaptations have been proposed, among which, vision fields, collision bias and group formation forces. From this type of model we will derive a macroscopic model in the next section.

A third, quite new, stream of models was proposed by the gaming industry. *Velocity-based models* simulate local operative movements (collision avoidance) by means of the optimization of time to collision with other pedestrians and objects at any point in time (Paris et al. (2007), Karamouzas and Overmars (2010), Moussaid et al. (2010)).

2.2.2. Macroscopic modelling approaches

Within macroscopic modelling approaches three modelling streams can be distinguished, being network models, hybrid models and continuum models. *Network models* solve crowd movement problems by means of mathematical approaches developed in graph theory (Chalmet and Saunders (1982), Lovas (1994), Daamen (2002)).

A second stream tries to incorporate the advantages of both microscopic and macroscopic modelling approaches (a.o. Banerjee et al. (2008), Xiong et al. (2010)). The two levels are either used in different spaces or time periods within the overall simulation, or combined sequentially (i.e the output of the first level gives input for the second level).

Finally, *Continuum models* simulate the global movement effects during which pedestrians are interpreted as particles of flow and PDE models are used to compute the solution. Hughes (2002) was the first to describe crowd movements by means of a continuous potential field approach, which is closely related to fluid dynamics. Several

studies have used hydrodynamic principles as the foundation for their simulation models (a.o. Treuille and Popovic (2006), Xiong et al. (2013), Jiang (2014)). In recent years, also macroscopic continuum models based on other principles have been proposed. Interactions of individuals among animal societies were used as inspiration of the Self-Organized Hydrodynamics model (Degond and Hua (2013)). Additionally, Cristiani et al. (2011) proposed a measure-based macroscopic model, and Rosini et al. (2011) discussed a model based on the Lighthill-Whithham and Richards (LWR) model (Colombo et al. (2011)). Schwandt et al. (2013) based their model on the principles of diffusion and convection. The microscopic principles of velocity-obstacle based models provided the basis for Degond et al. (2014). Each of these models uses the law of conservation of mass.

2.3. Modelling challenges

By definition, microscopic modelling approaches are very capable of simulating heterogeneous crowds. Yet, the computational effort required to operate these models for large crowds in any sizeable infrastructure is generally great. Therefore, computing optimal strategies remains a tedious endeavour.

Macroscopic models are not aimed at simulating the behaviour of individual pedestrians. However, when one requires a good estimation of the aggregate characteristics of crowd movements (i.e. velocity, density and flow), these models might provide useful predictions. Since the computational effort of macroscopic models is considerably lower than that of microscopic models, especially in situations where simulations need to be fast and not necessarily highly accurate, macroscopic models provide a good alternative. As such, the computation of optimal evacuation strategies and the operational management of large-scale pedestrian movement systems can benefit from the ongoing development of macroscopic models. Yet, as discussed previously, the macroscopic models proposed unto this moment are not capable of simulating all relevant behavioural processes and characteristics of crowds. For example, only a limited number of macroscopic models is capable of modelling bi-directional lane formation. The more sophisticated forms of (self-organizing) crowd movements, such as diagonal stripe formation in crossing flows, have not yet been simulated using macroscopic models, nor are we aware of macroscopic models that can capture the different phase transitions relevant for pedestrian flows.

3. Generic Multi-Class Pedestrian Flow Model

In this section, we present the model framework that will serve as a basis for the results presented in the remainder of this paper. The mathematical framework consists of the multi-class conservation equation, a specification of the equilibrium speed, and a specification of the equilibrium walking direction.

The model presented in this paper describes the dynamics of the class-specific density $\rho_d(t, \vec{x})$ over time t and space $\vec{x}$, where d denotes the pedestrian class. Here, the class describes the destination, whereby we assume that each pedestrian with the same destination behaves in the same way. In addition, other class definitions can be used as well, e.g. walking purpose, physical capabilities, gender, age group, etc. In many cases, a class would be determined by specific walking characteristics (e.g. desired walking speed, distances maintained to other pedestrians, etc.).

3.1. Conservation of pedestrian equation and equilibrium speed

The (class-specific) conservation of pedestrians equation for each class d is given by:

$$\frac{\partial \rho_d}{\partial t} + \nabla \cdot \vec{q}_d = r_d - s_d \tag{1}$$

where $\vec{q}_d$ denotes the two-dimensional flow vector; r_d and s_d respectively denote the source and sink terms. The source terms describe the inflow of pedestrians at the origin locations O_d, while the sink terms describe the outflow of pedestrians at the destination areas $\mathcal{D}_d$. The class-specific conservation of pedestrian equation shows how the density changes over time due to the longitudinal and lateral influx of pedestrians (expressed by $\nabla \cdot \vec{q}_d = \frac{\partial}{\partial x_1} q_{d,1} + \frac{\partial}{\partial x_2} q_{d,2}$).

Note that the continuity equation also holds for two dimensional pedestrian flows. For a two-dimensional pedestrian flow this implies that $\vec{q}_d = \rho_d \cdot \vec{v}_d$ where $\vec{v}_d = \vec{v}_d(t, \vec{x})$ is the mean velocity. This *velocity* is a two-dimensional vector that describes both the *(absolute) speed* u_d and the *direction* $\vec{\gamma}_d$ as a function of time t and location $\vec{x}$. Clearly, we have $u_d = \|\vec{v}_d\|$ and $\vec{\gamma}_d = \vec{v}_d / u_d$, and thus also $\vec{v}_d = \vec{\gamma}_d \cdot u_d$.

For the proposed model, we assume that the speed $u_d = \|\vec{v}_d\|$ satisfies (Hoogendoorn et al. (2014)):

$$u_d = U(\rho_1, ..., \rho_D, \nabla\rho_1, ..., \nabla\rho_D) \tag{2}$$

where U is the equilibrium speed, which is a function of the class-densities ρ_d and of the gradient of the class-specific densities $\nabla\rho_d$. In doing so, we are able to model the impacts of flow composition on the average walking speeds of a specific class. For pedestrian flows, only few studies on the shape of the fundamental diagram for multi-class flow operations have been performed (for instance, see Hoogendoorn and Bovy (2004a)); examples of multi-class fundamental diagrams for car traffic are described in Logghe and Immers (2008) and van Wageningen-Kessels et al. (2011).

For the sake of simplicity, in many cases we will assume $U = U(\rho)$ with $\rho = \sum_d \rho_d$. This implies that we assume that the total density determines the walking speed, irrespective of the compositions. Although this may not be a realistic assumption per se, it is less relevant for the main contribution of this paper, namely the realistic and dynamic modelling of walking direction and the resulting phenomena.

3.2. Walking direction modelling in continuous time and space

For the direction $\vec{\gamma}_d = \vec{v}_d/\|\vec{v}_d\|$ we put forward a specification that consists of a component that describes the global route choice behaviour and a component that describes the local choice behaviour. For the former, we recall previous work described by Hoogendoorn and Bovy (2004a), where the walking direction $\gamma_d(t, \vec{x})$ is determined using a dynamic programming approach. In this approach, the so-called *value function* $\phi_d(t, \vec{x})$ is determined by solving the Hamilton-Jacobi-Bellman equation; a global description is given in the next section. However, for details, we refer to Hoogendoorn and Bovy (2004b). The value function denotes the minimal cost (e.g. travel time, discomfort, or more generally effort) of getting from $(t, \vec{x})$ to destination d. Hoogendoorn and Bovy (2004b) show that if we know the minimum cost, we get for the optimum direction leading to the destination (under the assumption of invariant flow conditions):

$$\vec{\gamma}_d = -\frac{\nabla\phi_d}{\|\nabla\phi_d\|} \tag{3}$$

Note that $\phi_d(t, \vec{x})$ does not directly depend on the local densities $(\rho_1(t, \vec{x}), ..., \rho_D(t, \vec{x}))$ and can thus be considered to be exogenous. For any practical application, the value function will be computed prior to the simulation and will not be updated given prevailing flow conditions. It turns out, however, that this yields unrealistic predicted flow operations, where pedestrians will not consider to walk into low density areas that will provide them with a lower travel time, but rather stick to the path prescribed by the optimal direction $\vec{\gamma}_d(t, \vec{x})$. This potentially yields situations in which unnatural discontinuities occur in the direction perpendicular to the walking direction.

In illustration, consider a rectangular walking area Ω and a single class pedestrian flow. Assume that pedestrians walk from left to right, i.e. $\vec{\gamma}(t, \vec{x}) = (1, 0)$ for all $\vec{x} \in \Omega$. Boundary conditions are thus specified at the left boundary of the considered region (see Fig. 1). It is easy to see that the flow conditions can be determined by isolating a line with a fixed value for x_2 (e.g. $x_2 = y$ or $x_2 = y'$; see Fig. 1). On such a line, the combination of the (along the line one dimensional) conservation equation and the fundamental relation yields the one-dimensional kinematic wave model, that can be solved using well known techniques. Since the solutions for different lines $x_2 = y$ are independent of each other, discontinuities will occur in the lateral direction which is highly unrealistic.

Fig. 2 shows an numerical example illustrating the resulting traffic conditions in case only a global route choice model is considered. The simulations were performed using a linear fundamental diagram $U(\rho) = v_0 - \alpha_0\rho$ and a two dimensional extension of the Godunov scheme as applied in road traffic flow modelling (van Wageningen-Kessels et al., 2011). The numerical method used here and in the remainder of the paper is an improved version of the method proposed by Hänseler et al. (2014) and is expected to exhibit similar accuracy characteristics as the methods developed for one-dimensional road traffic (Daganzo, 1994; Lebacque, 1996). We have chosen the numerical settings (including time step size and grid cell size) such that numerical diffusion is minimised. In this test case, we have considered a single class pedestrian flow moving from left to right. The pedestrians enter the area Ω at $\vec{x} = (0, y)$ with $y = [-5, 5]$. Around $y = 0m$, we choose a higher demand than elsewhere on the boundary. We can clearly see that the lack of a density dependent direction choice factor causes the pedestrians to maintain the same lateral position, even

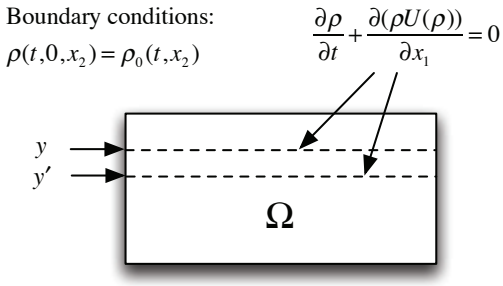

Fig. 1. Considered walking area Ω

if their direct neighbours move much faster. This holds for the pedestrians generated around $y = 0m$, as well as those generated at $y = \pm 5$.

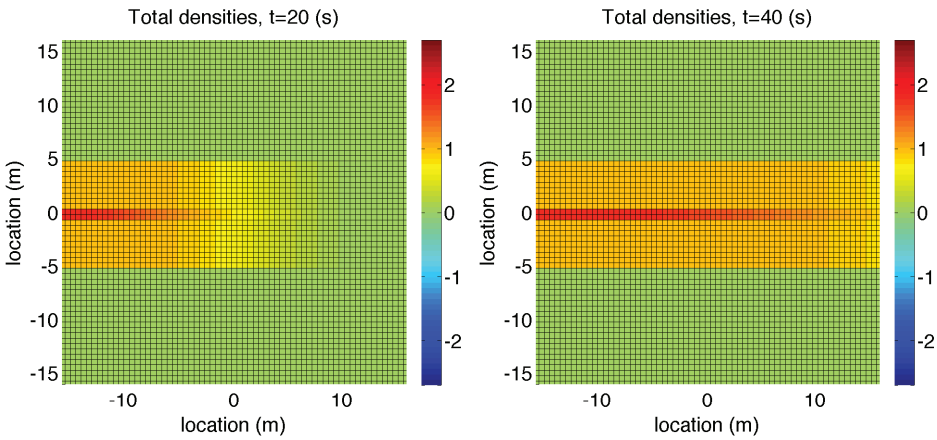

Fig. 2. Numerical experiment showing the impact of only considering global route choice on flow conditions.

To remedy these issues, in this paper we put forward a dynamic route choice model, that takes care of the fact that the global route choice behaviour is determined pre-trip and does not include the impact of changing flow conditions that may result in additional costs. To this end, we introduce a local route choice component that reflects additional local cost φ_d (e.g. extra delays, discomfort) caused by the prevailing flow conditions. We assume that these are dependent on the (spatial changes in the) class-specific densities.

In the remainder, we will assume that the local route cost function φ_d can be expressed as a function of the class-specific densities and density gradients. By differentiating between the classes, we can distinguish between local route costs incurred by interacting with pedestrians in the same class (walking into the same direction), and between class interactions. As a result, we have for the flow vector the following expression:

$$\vec{q}_d = \vec{\gamma}_d(\rho_1, ..., \rho_D, \nabla\rho_1, ..., \nabla\rho_D) \cdot \rho_d \cdot U(\rho_1, ..., \rho_D) \tag{4}$$

This expression shows that we will assume that the equilibrium speed is a function of the local densities of the respective classes, while the equilibrium direction is a function of both the densities and the density gradients. Note that this will make the model a *second-order model*, as we will discuss in the ensuing.

Finally, note that in assuming that initial and boundary conditions are known, eqn. (1) and (4) together give a complete mathematical model allowing us to determined the dynamics. Furthermore, the function U should be known, as discussed before. The local route choice function $\vec{\gamma}$ will be discussed in the next section.

4. Local value function definition and application

In this section, we propose a novel specification for the local route choice model based on the assumption that people will locally minimise their travel cost. We first present the generic multi-class model specification, including the specification of the global and the local route choice model. We next briefly recall the work presented in Hoogendoorn et al. (2014), where we derived a local route choice model from microscopic pedestrian interaction models, and show how this is a special case of the model presented here. Next, we further specify the local route choice model, including both crowdedness and delay factors.

4.1. Generic local route choice using the local value function

As was mentioned in the previous section, global route choice and local route choice are combined by adding a local value function φ_d, which describes the impact of the local conditions on the cost of reaching the destination, to the global value function ϕ_d describing the minimum cost of getting from point $(t, \vec{x})$ to any of the relevant destinations for pedestrians in class d:

$$\phi_d(t, \vec{x}) = \min_{\vec{v}_{[t,T)}} E\left\{\int_t^T L(s, \vec{x}(s), \vec{v}(s))ds + \theta_d(T, \vec{x}(T))\right\} \tag{5}$$

subject to the stochastic differential equation:

$$d\vec{x} = \vec{v}dt + \varepsilon d\xi \tag{6}$$

where ξ is a zero-mean noise term that describes the uncertainty in the outcome (location) when applying a velocity; L is the so-called running cost - the cost the pedestrian incurs in a short interval $[t, t + dt)$ when he is at location $\vec{x}$ and moves with velocity $\vec{v}$. The function $\theta_d(T, \vec{x}(T))$ denotes the terminal cost - i.e. the cost of arriving at the destination $\mathcal{D}_d$ before the terminal time T. For more details and numerical solution approaches, we refer to Hoogendoorn and Bovy (2004a,b).

This global value function $\phi_d(t, \vec{x})$ can be computed by solving the so-called Hamilton-Jacobi-Bellman equation:

$$\frac{\partial \phi_d}{\partial t} + H(t, \vec{x}, \nabla\phi_d, \Delta\phi_d) = 0 \tag{7}$$

with the Hamiltonian given by:

$$H(t, \vec{x}, \nabla\phi_d, \Delta\phi_d) = \min_{\vec{v}\in\mathcal{V}_d} \{L(t, \vec{x}, \vec{v}) + \nabla\phi_d \cdot \vec{v} + \varepsilon\Delta\phi_d\} \tag{8}$$

with $\phi_d(T, \vec{x}(T)) = \theta_d(T, \vec{x}(T))$. This equation allows us to compute the global value function using dedicated computational techniques. Note that the set $\mathcal{V}_d$ denotes the admissible velocities (i.e. admissible speeds and directions), that can be applied by a pedestrian, given physical abilities, infrastructure layout, etc. Let us emphasise that although we assume uncertainty in the path that a pedestrian will take when a certain velocity is applied (Eqn. (6)), the fact that we consider minimum *expected* cost result in a deterministic system, where the impact of uncertainty is reflected only by the diffusion term in the Hamiltonian (Eqn. (8)).

Let us note that *in principle*, anticipated changes in the density and the impact thereof during the planning interval $[t, T)$ can in principle be dealt with, as is discussed in Hoogendoorn and Bovy (2004a). Next to the fact that this turns out to be computationally cumbersome, it is also rather unrealistic to assume that pedestrians can predict precisely where higher density areas will be during the entire planning period.

This is why we have opted to introduce the local value function φ_d, reflecting additional walking cost because of local (unforeseen) fluctuations in the density. These local cost can stem from local delays, or from the fact that costs are incurred when pedestrians walk in a region where the level of service is low due to high densities.

We will define this function in such a way that the following will hold:

$$\nabla\varphi_d = \sum_{\delta=1}^{D}\left\{\beta_\delta - \alpha_d\eta_\delta\frac{1}{\tilde{U}(\tilde{\rho})^2}\frac{d\tilde{U}}{d\tilde{\rho}}\right\}\cdot\nabla\rho_\delta = \sum_{\delta=1}^{D} f_\delta(\tilde{\rho})\cdot\nabla\rho_\delta \tag{9}$$

Here, $\tilde{U}$ describes the perceived walking speed as a function of the local effective density $\tilde{\rho}$. This expression shows how the gradient of the local value function for pedestrians of group d is a weighted sum of the density gradients of the densities ρ_δ of the different pedestrian classes δ. The non-linear weights $f_\delta(\tilde{\rho})$ describe to which extent these density gradients contribute to the overall gradient and thus to the local route choice.

In combining the global and local route choice, we simply add the global and local value function into the overall value function $\omega_d = \phi_d + \varphi_d$. The resulting direction choice model that follows from this choice is given by Eqn. (20).

Before deriving Eqn. (9), we briefly recall the result from Hoogendoorn et al. (2014), where we derived a local route choice model from microscopic pedestrian interaction models. The model that results from this approach can be recast in a local value function formulation, as will be shown in the ensuing.

4.2. Local value function from microscopic principles

In Hoogendoorn et al. (2014), the local route choice was determined from repelling microscopic interactions stemming from microscopic pedestrian models, such as the social-forces model described by Helbing and Molnar (1995). Without going into detail here, the resulting macroscopic direction choice model can be described by defining the local value function φ_d as follows:

$$\varphi_d = \sum_{\delta=1}^{D} \beta_\delta \rho_\delta \tag{10}$$

where β_δ is some constant value that depends on the parameters of the chosen microscopic interaction model. This leads to the following route choice model:

$$\vec{\gamma}_d = -\frac{\nabla\phi_d + \sum_{d'} \beta_{d'} \cdot \nabla\rho_{d'}}{\|\nabla\phi_d + \sum_{d'} \beta_{d'} \cdot \nabla\rho_{d'}\|} = \frac{\vec{v}_0 - \sum_{d'} \beta_{d'} \cdot \nabla\rho_{d'}}{\|\vec{v}_0 - \sum_{d'} \beta_{d'} \cdot \nabla\rho_{d'}\|} \tag{11}$$

This expression shows how the global route choice, expressed in by the desired velocity $\vec{v}_0(t, \vec{x})$ is influenced by the local route choice model, that is determined by the gradient of the density of the respective user-classes. Note that in the approach of Hoogendoorn et al. (2014), also the speed u_d depends on the density gradient. This may lead to unrealistic properties of the speed - density relation (i.e. negative speeds in case of high densities combined with large density gradients or speeds (much) larger than predefined free flow speeds in case of low densities and large density gradients). In this paper we only consider the impact of spatially distinct flow conditions on the local route cost and hence on the flow direction.

4.3. Specification of local value function based on local delays

In this section, we propose an alternative model for the local value function that directly stems from the principle that also underlies the global route choice model, namely that pedestrians aim to minimise the cost of getting to their destination. To do this, let us assume that the cost is the (generalised) travel time of getting from the current location $\vec{x}(t)$ to the destination area $\mathcal{D}_d$. To this end, the local value function φ_d expresses the additional (perceived) local travel costs that is incurred due to the fact that the density is higher (or lower) than expected (as reflected by the global value function).

The local cost for a pedestrian of group d can stem from different factors. The most simple specification follows when assuming that pedestrians tend to avoid high density areas, in particular if these high densities are made up of pedestrians from other classes. Assuming that these costs are linear with respect to the densities yields a specification equal to Eqn. (10). In this case, the values β_δ can be interpreted as weights that a pedestrian of group d attaches to densities of his own ($\delta = d$) and of other classes ($\delta \neq d$). In the remainder, we refer to this component of the local walking cost by $\varphi_d^{crowdedness}$.

Another specification stems when looking at local delays caused by reduced walking speeds due to high densities. To this end, consider a pedestrian walking into a certain direction for a very short time interval $[t, t + dt)$. The delay this pedestrian incurs during the interval is equal to:

$$\lambda_d(\rho_1, ..., \rho_D)dt = \left(\frac{1}{\tilde{U}(\rho_1, ..., \rho_D)} - \frac{1}{\tilde{U}(0)}\right)dt \tag{12}$$

where the density is assessed along the direction in which the pedestrian in walking. The function $\tilde{U}$ is a function of the densities ρ_δ and reflects the perceived walking speed of a pedestrian in class d. In the remainder, we will assume that the function $\tilde{U}$ can be expressed as a function of the *effective density* $\tilde{\rho}$ defined by:

$$\tilde{\rho} = \sum_{\delta=1}^{D} \eta_\delta \cdot \rho_\delta \tag{13}$$

The weights η_δ reflect the (perceived) contribution of the density of group δ to the effective density, and as such to the reduction in the perceived walking speed. This motivates us to define the local value function as follows:

$$\varphi_d^{delay} = \lambda_d(\tilde{\rho}) \tag{14}$$

Note that the term is directly related to the local pace (i.e. the inverse of the speed).

Although other specifications of the local cost (or local value function) are possible, in the remainder, we assume that the local value function φ_d for pedestrians of group d is the weighted sum of the two terms proposed above:

$$\varphi_d = \varphi_d^{crowdedness} + \alpha_d \cdot \varphi_d^{delay} \tag{15}$$

where α_d is the weight that can be used to influence the relative importance of the two factors. Note that the two components describe different behavioural mechanisms, which justifies their distinction: while the crowdedness component describes the tendency to move to less dense areas (which may result in a small detour), the delay component describes the aim to choose a (local) route with the shortest travel time. Although it is plausible that both terms will play a role in pedestrian behaviour, extensive data analysis and model estimation studies would be required to see the relative importance of both terms in reality. In this paper, we only consider their impact on the resulting macroscopic flow patterns.

The local direction choice is dependent on the gradient of the local value function φ_d. Clearly, we have:

$$\nabla\varphi_d = \nabla \cdot \varphi_d^{crowdedness} + \alpha_d \cdot \nabla\varphi_d^{delay} \tag{16}$$

For the *crowdedness factor*, we get:

$$\nabla\varphi_d^{crowdedness} = \sum_{\delta=1}^{D} \beta_\delta \cdot \nabla\rho_\delta \tag{17}$$

Clearly, the term $\nabla\rho_\delta$ shows how pedestrians will move into areas in which the density of pedestrians of group δ is the smallest. The extent to which this happens depends on the weight β_δ. If the classes indicate groups of pedestrians with different origins or destinations, but with for the rest the same characteristics, we can assume that $\beta_\delta \geq \beta_d$ for $\delta \neq d$; in other words, pedestrians will try to avoid pedestrians of other groups harder than pedestrians of their own group.

For the *delay factor*, we get:

$$\nabla\varphi_d{}^{delay} = \nabla\lambda_d(\tilde{\rho}) = \sum_{\delta=1}^{D} \frac{d\lambda_d}{d\tilde{\rho}} \cdot \frac{\partial\tilde{\rho}}{\partial\rho_\delta} \cdot \nabla\rho_\delta = \frac{d\lambda_d}{d\tilde{\rho}} \cdot \sum_{\delta=1}^{D} \eta_\delta \cdot \nabla\rho_\delta \tag{18}$$

We can easily show that:

$$\frac{d\lambda_d}{d\tilde{\rho}} = -\frac{1}{\tilde{U}(\tilde{\rho})^2}\frac{d\tilde{U}}{d\tilde{\rho}} \geq 0 \tag{19}$$

Eqns. (18) and (19) show that for the delay component the local cost function changes the walking direction according to the (weighted) density gradient $\nabla\rho_\delta$, and the increase in the travel time given the prevailing traffic conditions which is expressed by $d\lambda_d/d\tilde{\rho}$. Eqn. (19) shows that the latter value can become very large in case the densities are very high (near jam density) and $U(\rho)$ is nearly zero. This means that pedestrians will avoid dense areas, and that this avoidance becomes stronger when the density becomes higher.

Combining the two terms leaves us with the generic expression proposed by Eqn. (9).

4.4. Combining global and local route choice

As was proposed in the previous section, the new model uses the composite value function $\omega_d = \phi_d + \varphi_d$ to determine the walking direction via:

$$\vec{\gamma}_d = -\frac{\nabla\omega_d}{||\nabla\omega_d||} = -\frac{\nabla\phi_d + \nabla\varphi_d}{||\nabla\phi_d + \nabla\varphi_d||} \tag{20}$$

Note that implicitly, weighing of the two terms is applied via the parameters of the local value function. Using Eq. (4), the conservation of pedestrian equation Eq. (1), and the speed-density relation $u_d = U(\rho)$, results in the newly developed model.

In the remainder of the paper, we investigate the properties of the proposed model, in particular focussing on self-organisation and the failure thereof.

5. Simulation experiments

In this section we illustrate some of the properties of the newly developed model. We first show the impact of including local route choice on the dispersion of pedestrians. Secondly, we show under which conditions the model predicts the formation of self-organised patterns, in particular diagonal stripe formation and bi-directional lane formation. To this end, we investigate the influence of class-specific cost factors (i.e. interactions with other classes results in different local costs than with other classes). Thirdly, we investigate to which extent the new model can capture the breakdown of self-organisation. For all our simulations we use the Godunov scheme, as described in Section 3.2.

Next to this, we investigate the impacts of the different terms in the model. In particular, we look at the impact of differences in the weights β_δ (and η_δ) that describe the relative impact of the densities of the other groups compared to the density of the own group. Finally, we look at the relative impacts of the crowdedness terms and the delay term via changing the parameter α_d.

5.1. Introducing the base model and the scenarios

Our base model is defined by using a linear speed-density relation $U(\rho) = v_0 \cdot (1 - \rho/\rho_{jam}) = 1.34 \cdot (1 - \rho/5.4)$. We choose this relation for its simplicity, being fully aware that more realistic relations better fitting real data have been put forward in literature. Since in this paper we aim to show the qualitative properties of the model, we choose simplicity over realism. Furthermore, we use $\beta_\delta = \eta_\delta = 1$ for $\delta = d$ and $\beta_\delta = \eta_\delta = 4$ otherwise, meaning that the impact of the densities of the other groups are substantially higher than the impact of a pedestrian's own group. Finally, in the base model we only consider the impact of the crowdedness factor, i.e. $\alpha_d = 0$; the impact of the delay terms is considered separately in section 5.6.

To test the base model, and the different variants on it, we use three scenarios:

1. *Unidirectional flow scenario*, mostly used to show flow dispersion compared to the example presented in section 3.2. In this scenario, pedestrians enter on the left side of the fourty by fourty meter area and walk towards the right.
2. *Crossing flow scenario*, where the first group of pedestrians is generated on the left, and walks to the right, while the second group is generated at the bottom of the area, and moves up.
3. *Bi-directional flow scenario*, where two groups of pedestrians are generated at respectively the left and the right side of the fourty by fourty meter area and walk towards the opposite side.

In all scenarios, pedestrians are generated on the edges of the area between $-5m$ and $5m$.

5.2. Impact of local route choice of flow dispersion

Let us first revisit the scenario presented in section 3.2, shown in Fig. 1. The example considered a uni-directional pedestrian flow with fixed (global) route choice. The resulting flow operations showed no lateral dispersion of pedes-

trians, which appears to be not realistic since it caused large differences in speeds and travel times for pedestrians that are spatially very close.

Including the local choice term φ_d causes dispersion in a lateral sense: since pedestrians avoid high density areas, densities will disperse and smooth over the area, see Fig. 3. The resulting flow conditions appear much more realistic than the situation that occurred in case the local route choice model was not included.

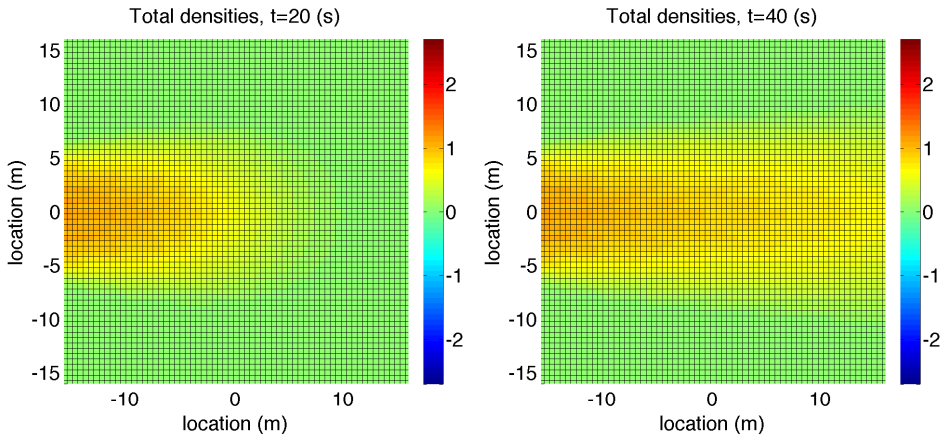

Fig. 3. Numerical experiment showing the impact of only considering global route choice on flow conditions. For the simulations, we have used a linear fundamental diagram $U(\rho) = v_0 - \alpha_0\rho$.

5.3. Self-organisation characteristics for crossing and bi-directional flows

To show the ability of the model to reproduce self-organised patterns in pedestrian flows, let us first consider the crossing flow scenario. We consider a situation where the demand is $0.12P/m/s$. We consider the base model, for both scenarios 2 and 3.

The simulation shows the formation of self-organised structures, i.e. diagonal stripes. The stripes that are formed move through each other in the region where the two flows intersect. The stripes move at a certain speed and result in a reasonably efficient flow. Fig. 4 shows some of the results. The left part of the figure shows the stable end result for the pedestrians walking from left to right (the other direction shows a similar picture). The right part of the picture shows the outflow of the area (for both groups). Note that the outflow rate is scaled against the demand.

The results clearly show that the base model is able to reproduce self-organisation. The model seems to be able to describe a spontaneous phase transition from a normal situation to the self-organised patterns that can be seen in the picture. We can also see from the figure (right) that during the transition, the outflow reduces temporarily. This also means that a certain amount of pedestrians is stored in the area. Also note that the outflow characteristics are changing form a very stable outflow to a high frequency oscillatory outflow pattern. Nevertheless, the average outflow is equal to the demand.

Let us note that we also tested the model *without the local route choice*. In this case, the only mechanism that determines the direction is the global route choice, which essentially determines the shortest path under free flow conditions towards the destination. Although the speeds will depend on the (total) density of the two crossing flows, there is no incentive for the pedestrians to move towards an area which is either less dense or in which pedestrians walking in the same direction are walking. The simulation results (not shown) do not reveal any type of self-organised patterns, which provides experimental evidence that the self-organisation is indeed caused by including local route choice.

It turns out that the model is also able to reproduce the formation of dynamic lanes in bi-directional flows. Fig. 5 shows the results, again assuming a demand of $0.12P/m/s$. The left figure shows the initiation of the lane formation process occurring at around $130s$ (a similar pattern occurs for the other direction). The patterns that we observe are resemblant of the dynamic lanes that have been shown to form in empirical bi-directional flows. Note that similar to

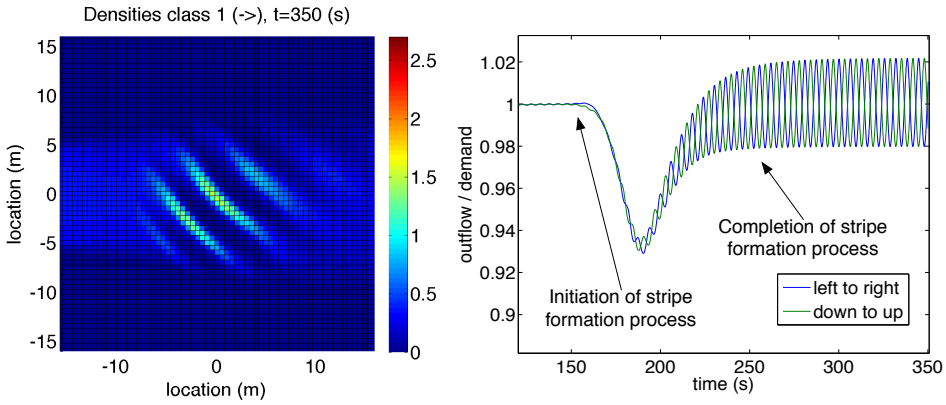

Fig. 4. Density contour plot (left) and scaled outflow rate (right) for crossing flows.

the crossing flow scenario, after some time, the situation stabilises. However, the demand - outflow ratio stays below one. This is due to the fact that pedestrians walking in the opposite direction cannot enter the area at the location where the pedestrians that have formed the lane are exiting.

Also for the bi-directional case, we tested the model without the local route choice. The simulation results (not shown) again do not reveal any type of self-organised patterns, providing also for this case experimental evidence that the self-organisation of bi-directional lanes is indeed caused by including local route choice.

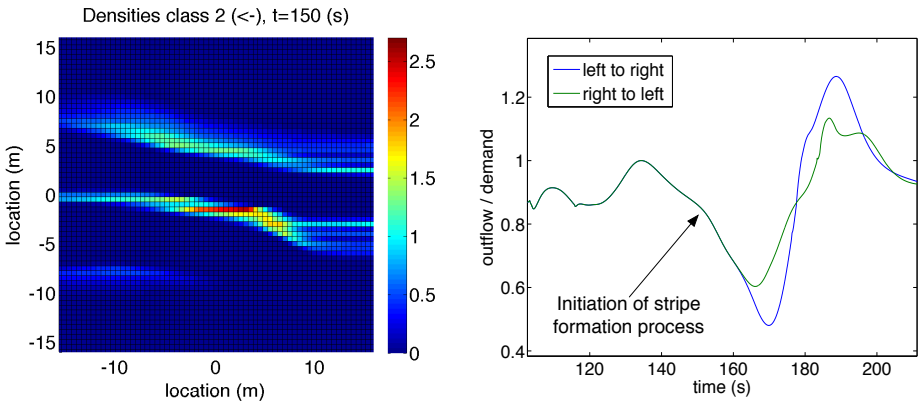

Fig. 5. Density contour plot (left) and scaled outflow rate (right) for bi-directional flows.

Based on the results presented here, it is safe to conclude that the proposed model is able to reproduce self-organised patterns. That is, the model is not only able to more realistically capture flow dispersion, as was shown in the previous section, it also captures other key phenomena characterising pedestrian flows, at least qualitatively.

5.4. Influence of demand on self-organised patterns

In the preceding, we have seen how the proposed model is able to capture self-organisation. Let us now briefly investigate what the impact of the demand is on this process. To this end, we consider the crossing flow scenario.

Fig. 6 shows the results of four demand scenarios, defined by respectively demands of 0.10, 0.15, 0.18, and 0.25 P/m/s. We can clearly see how the demand influences the self-organised patterns that are formed. For low demands (0.1 P/m/s), no self-organised patterns occur: the resulting densities are sufficiently low implying that there is sufficient room to simply pass through the other flow without the need to form structures to increase efficient interaction.

For higher demands, we see self-organised patterns. Until a demand of say 0.18 P/m/s, we see diagonal stripe formation. However, if the demand becomes too large, the neat self-organisation seen at lower demand scenarios seems to fail. We still see forms of self-organisation, where pedestrians walking into a certain direction are clustered in homogeneous groups that move as a block through the other classes. If the demand increases further, the process stagnates completely and a full gridlock results.

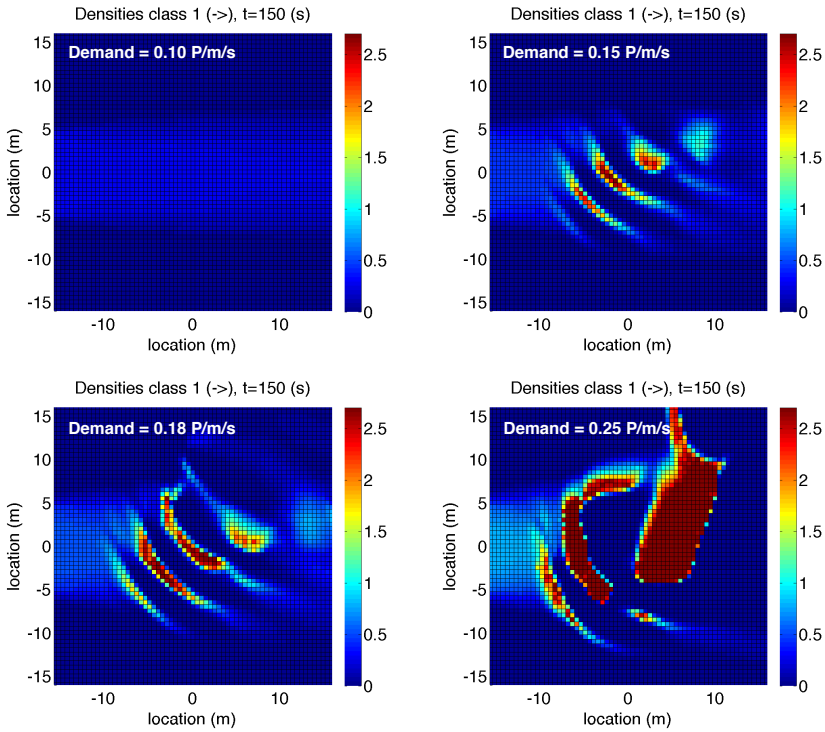

Fig. 6. Density contour plot with different inflow demands.

To illustrate this process further, we have determined the average outflow of the area for both considered directions (again, scaled to demand to ensure that we can compare the different scenarios). Fig. 7 shows the results of this experiment: note that the average flow for the considered 400 s simulation period is never equal to 1, even if the demand is very small. The reason is that we considered the average outflow for the entire simulation period, including the start-up period where the outflow is still zero.

The figure shows clearly how self-organisation and the failing thereof impacts the efficiency of the process: from the moment that the demand exceeds 0.18 P/m/s, the outflow / demand ratio decreases strongly with increasing demand. Also note that between 0.22 P/m/s ad 0.38 P/m/s, the demand - outflow relation appears more erratic, showing that still some self-organised patterns occur that sometimes leads to (temporary) reasonable efficient flow. From demands of 0.38 P/m/s onward, the outflow completely stagnates and a grid-lock situation occurs.

Based on these simulation results, we may conclude that the self-organisation that the model reproduces depends strongly on the demand levels considered: if demand is too low, self-organisation does not occur; if demand is too high, self-organisations stagnates and flow efficiency is substantially reduced. Again, the results seem realistic compared to empirical knowledge about self-organised phenomena in pedestrian flows, at least from a qualitative perspective.

5.5. Influence of weight factors on model behaviour

The choice of the β_δ (the weight of the densities of other classes compared to the weight of the pedestrian's own class) turns out to have a very profound impact on the model behaviour. In illustration, we considered the case when $\beta_\delta = 1$ and $\beta_\delta = 2$ (instead of 4) for $\delta = d$ and $\delta \neq d$ respectively. For this choice of weights, self-organisation occurs

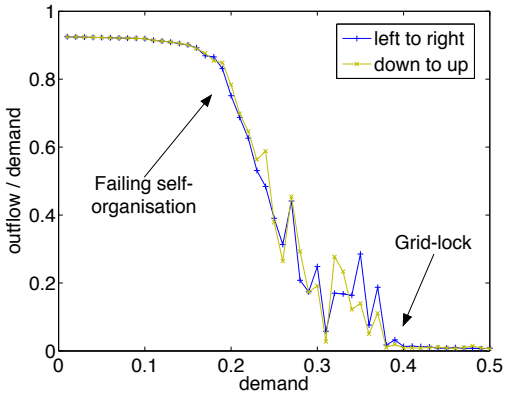

Fig. 7. Average outflow of the area for both walking directions as a function of the demand.

only at much higher demands (i.e. larger than 0.3 P/m/s). Fig. 8 (left) illustrates this by showing the normalised outflow.

Considering larger values for β_δ for $\delta \neq d$ provides just the opposite result: the formation of diagonal stripes occurs earlier (at a demand of 0.1 P/m/s), as does the failure of self-organisation process (at a demand of 0.3 P/m/s), see Fig. 8 (right). Both examples clearly illustrate the impact of the weights β_δ on the model characteristics.

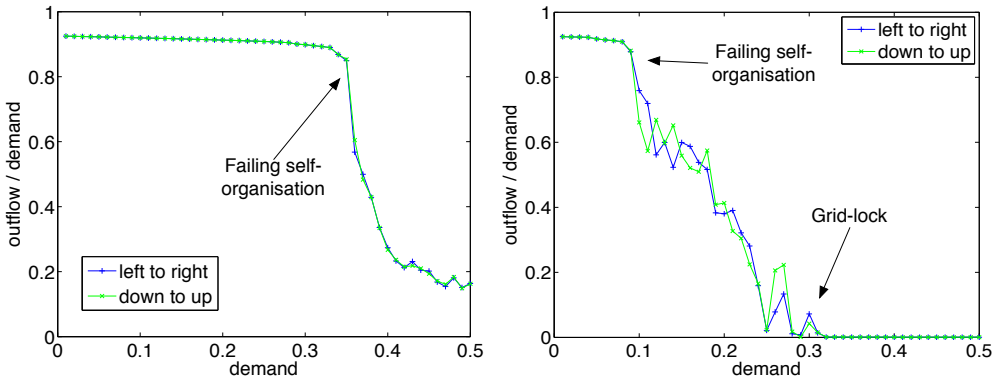

Fig. 8. Relation between demand and normalised outflow for $\beta_\delta = 2$ for $\delta = d$ (left) and for $\beta_\delta = 8$ for $\delta = d$

.

5.6. *Influence of delay factor on model behaviour*

So far, we have considered the impact of the crowdedness factor on the model behaviour. In this final experiment, we investigate the impact of the delay factor. Examining Eqn. (9) shows that contrary to the crowdedness factor, the delay factor yields a non-linear, effective density dependent weight factor.

For a linear perceived speed-density function, we have $d\tilde{U}/d\tilde{\rho} = -v^0/\rho_{jam}$. Since the weight scales with $1/\tilde{U}^2$, the influence of the density gradients will be smaller for lower densities than for higher densities. This means that for low densities, pedestrians will have very little incentive to adapt their path; for high densities, they will be much more inclined to do so. The crowdedness factor has constant weights, which means that the inclination to change direction will be the same for low and high densities, which arguably is not very realistic.

Fig. 9 shows the relation between the demand and the normalised outflow for a case where $\eta_\delta = 1$ for $\delta = d$ and $\eta_\delta = 4$ for $\delta \neq d$. The fact that the weighting of the density gradients is dependent on the density (i.e. in case

of only considering the delay factor) causes that self-organisation occurs at higher demands (and densities) than in case of constant weights (i.e. in case of only considering the crowdedness factor). Moreover, the figure shows that although self-organisation will occur, it also quickly fails causing the outflow to reduce to a very low value. In fact, self-organisation only occurs for demands between say 0.2 P/m/s and 0.3 P/m/s.

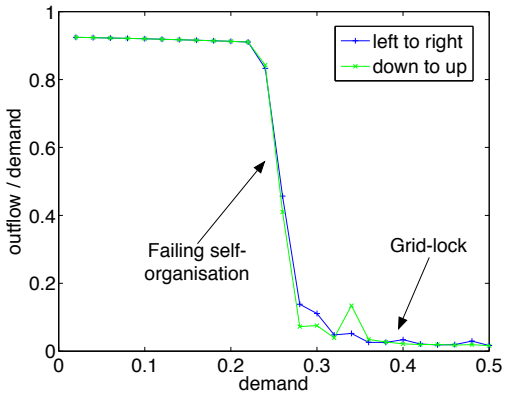

Fig. 9. Relation between demand and outflow for delay factor.

In illustration, Fig. 10 shows a snapshot of the self-organised pattern (left) as well as the normalised outflow as a function of time (right) for a demand of 0.24 P/m/s. For this demand scenario, we observe that the self-organisation of diagonal stripes occurs for a very short period of time, after which it breaks up, and outflow stagnates. This on the contrary to the model where only the crowdedness factor is considered (as show in the previous examples), where the self-organised patterns are stable for certain demands.

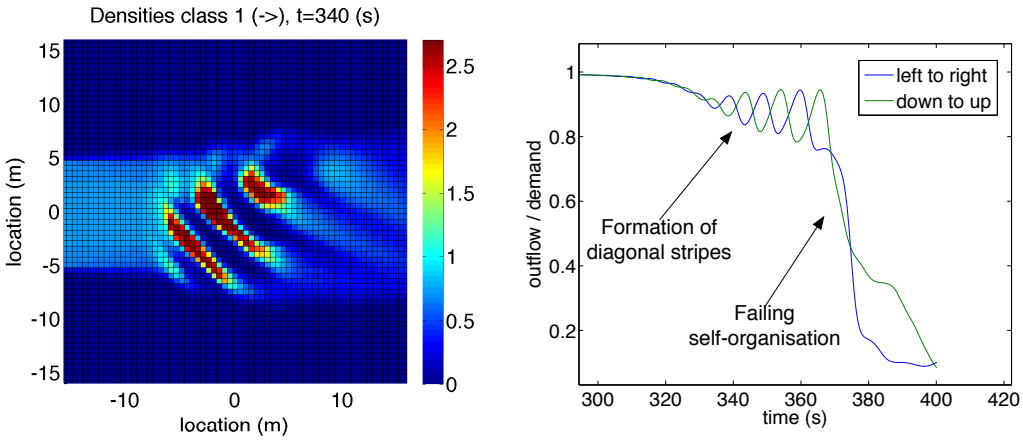

Fig. 10. Self-organisation of diagonal stripes for demand of 0.24 P/m/s.

6. Conclusions

In this paper, we proposed a macroscopic multi-class pedestrian model. The basis of the model is a two-dimensional conservation of pedestrians equation. Similar to the kinematic wave model for vehicular traffic, the speeds of the pedestrians belonging to a specific class, which in our case are pedestrians with a certain destination, is given by an equilibrium speed-density relation.

The main contribution of the paper is the proposed model for the equilibrium direction of the pedestrians, which is governed by two parts: one part describing the global route choice, which is pre-determined based on the expectations

of the pedestrians, and one part describing the local route choice, which is a density-gradient dependent term that reflects local adaptations based on prevailing flow conditions.

The local route choice is in turn governed by two factors: one reflecting the pedestrian's tendency to move away from high-density areas (crowdedness factor), and one describing the expected increase in delay caused by local densities (delay factor). Including the local route choice is done via the local value function, describing the increase in the global cost of getting from the current location to the destination.

Including the local route choice term in the multi-class model causes first of all dispersion of the flow: pedestrians will move away from high density areas in order to reduce their overall walking costs. Second of all, for the crossing flow and bi-directional flow cases, local route choice causes well known self-organised patterns to emerge (i.e. diagonal stripes and bi-directional lanes). We have studied under which demand conditions self-organisation occurs and fails, as well as what the impact is of the choices of the different model parameters. In particular, the differences in the weights reflecting the impact of the own and the other classes appears to have a very strong impact on the self-organisation process.

Furthermore, we have considered the differences in model characteristics when including the crowdedness factor and the delay factor, which turn out to be considerable. In particular, the density dependent weights that stem from the delay factor cause self-organisation to occur only within a very limited demand range. Also, the (efficient) self-organised patterns (e.g. diagonal stripes) occur only for a short period of time, that is, they are not stable. More research is required to determine which of the two terms, the crowdedness or the delay, or a combination of both, yields the most realistic results.

7. Acknowledgements

This research is performed as part of the NWO-VICI project "Travel Behavior And Traffic Operations In Case Of Exceptional Events" (Hoogendoorn), and as part of the NWO Aspasia grant of Daamen (Daamen, Van Wageningen-Kessels).

References

Banerjee, B., Abukmail, A., Kraemer, L., 2008. Advancing the layered approach to agent-based crowd simulation. Proceedings of the IEEE Workshop on Parallel and Distributed, Simulation , 185–192.

Blue, V., Adler, J., 1998. Emergent fundamental pedestrian flows from cellular automata microsimulation. Transportation Research Record 1644, 29–36.

Blue, V., Adler, J., 2001. Cellular automata microsimulation for modeling bi-directional pedestrian walkways. Transportation Research Part B: Methodological 35, 293–312.

Camazine, S., Deneubourg, J.L., Franks, N., Sneyd, J., Theraulax, G., Bonabeau, E., 2010. Self-Organisation in Biological Systems. Princeton University Press.

Chalmet, L.G., R.F., Saunders, P., 1982. Network models for building evacuation. Management Science 28, 86–105.

Chattaraj, U., Seyfried, A., Chakroborty, P., 2009. Comparison of pedestrian fundamental diagram across cultures. Advances in Complex Systems 12, 393–405.

Colombo, R., Garavello, M., Lecureau-Mercier, M., 2011. Non-local crowd dynamics. Comptes Rendus Mathematique 349 (13-14), 769–772.

Cristiani, E., Piccoli, B., Tosin, A., 2011. Multiscale modeling of granular flows with application to crowd dynamics. Multiscale Modeling and Simulation 9, 155–182.

Daamen, W., 2002. Simped: a pedestrian simulation tool for large pedestrian areas, in: Conference proceedings EuroSIW, 24-26 June 2002.

Daganzo, C.F., 1994. The cell transmission model: A dynamic representation of highway traffic consistent with the hydrodynamic theory. Transportation Research Part B: Methodological 28, 269–287. URL: http://www.sciencedirect.com/science/article/B6V99-466CFRH-98/2/51992b6da4383e0faf83a17023eb2f01, doi:DOI: 10.1016/0191-2615(94)90002-7.

Degond, P., Appert-Rolland, C., Pettre, J., Theraulaz, 2014. Vision-based macroscopic pedestrian models. Kinetic and Related Models 6(4), 809–839.

Degond, P., Hua, J., 2013. Self-organized hydrodynamics with congestion and path formation in crowds. Journal of Computational Physics .

Duives, D., Daamen, W., Hoogendoorn, S., 2013. State-of-the-art crowd motion simulation models. Transportation Research Part C: Emerging Technologies 37, 193 – 209.

Hänseler, F.S., Bierlaire, M., Farooq, B., Mühlematter, T., 2014. A macroscopic loading model for time-varying pedestrian flows in public walking areas. Transportation Research Part B: Methodological 69, 60–80. URL: http://www.sciencedirect.com/science/article/pii/S0191261514001386, doi:http://dx.doi.org/10.1016/j.trb.2014.08.003.

Helbing, D., Buzna, L., Johansson, A., Werner, T., 2005. Self-organized pedestrian crowd dynamics: experiments, simulations, and design solutions. Transportation Science 39, 1–24.

Helbing, D., Johansson, A., 2010. Pedestrian, crowd and evacuation dynamics. Encyclopedia of complexity and System Science 16, 6476–6495.

Helbing, D., Johansson, A., Al-Abideen, H.Z., 2007. Dynamics of crowd disasters: An empirical study. Physical Review E 75, 046109.

Helbing, D., Molnar, P., 1995. Social force model for pedestrian dynamics. Physical Review E 51, 4282–4286.

Hoogendoorn, S., Daamen, W., 2004. Self-organization in walker experiments, in: Proceedings of the 5th Symposium on Traffic and Granular Flow, pp. 121–131.

Hoogendoorn, S., Daamen, W., 2005. Pedestrian behavior at bottlenecks. Transportation Science 39, 147–159.

Hoogendoorn, S., van Wageningen-Kessels, F.L.M., Daamen, W., Duives, D.C., 2014. Continuum modelling of pedestrian flows: From microscopic principles to self-organised continuum modelling of pedestrian flows: From microscopic principles to self-organised macroscopic phenomena. Physica A .

Hoogendoorn, S.P., Bovy, P.H., 2004a. Dynamic user-optimal assignment in continuous time and space. Transportation Research Part B: Methodological 38, 571–592.

Hoogendoorn, S.P., Bovy, P.H., 2004b. Pedestrian route-choice and activity scheduling theory and models. Transportation Research Part B: Methodological 38, 169–190.

Hoogendoorn, S.P., Daamen, W., van Wageningen-Kessels, F.L.M., 2013. Optimal crowd evacuation, in: Transportation Research Board Annual Meeting Preprints.

Hughes, R., 2002. A continuum theory for the flow of pedestrians. Transportation Research Part B: Methodological 36, 507–535.

Jiang, Y., 2014. Evacuation modeling of pedestrian flow considering the herd behavior. Applied Mechanics and Materials 444-445, 906–911.

Karamouzas, I., Overmars, M., 2010. A velocity-based approach for simulating human collision avoidance. volume 6356. pp. 180–186.

Lebacque, J.P., 1996. The Godunov scheme and what it means for first order traffic flow models, in: Lesort, J.B. (Ed.), Transportation and Traffic Theory: Proceedings of the 13th International Symposium on Transportation and Traffic Theory, 1996, Pergamon. pp. 647–677.

Logghe, S., Immers, L., 2008. Multi-class kinematic wave theory of traffic flow. Transportation Research Part B: Methodological 42, 523–541.

Lovas, G., 1994. Modeling and simulation of pedestrian traffic flow. Transportation Research Part B: Methodological 28B, 429–433.

Moussaid, M., Perozo, N., Garnier, S., Helbing, D., Theraulaz, G., 2010. The walking behavior of pedestrian social groups and its impact on crowd dynamics. PLoS ONE 5, e10047.

Navin, F., Wheeler, R., 1969. Pedestrian flow characteristics. Traffic Engineering 39, 3036.

Oeding, D., 1963. Verkehrsbelastung und dimensionierung von gehwegen und anderen anlagen des fugngerverkehrs. Straenbau and Straenverkehrstechnik 22. (In German).

Paris, S., Pettre, J., Donikian, S., 2007. Pedestrian reactive navigation for crowd simulation: a predictive approach, in: Cohen-Or, D.P.S. (Ed.), Eurographics 2007, Computer Graphics Forum. pp. 665–674.

Schadschneider, A., Klingsch, W., Klpfel, H., Kretz, T., Rogsch, C., Seyfried, A., 2009. Encyclopedia of Complexity and Systems Science. Springer New York. chapter Evacuation Dynamics: Empirical Results, Modeling and Applications. pp. 3142–3176.

Schwandt, H., Huth, F., Barwolff, G., 2013. A macroscopic model for intersecting pedestrian streams with tactical and strategical redirection. AIP Conference Proceedings 1558, 2209.

Treuille, A., S.C., Popovic, Z., 2006. Continuum crowds. ACM Transportation Graphics 25, 1160–1168.

van Wageningen-Kessels, F.L.M., van 't Hof, B., Hoogendoorn, S.P., Vuik, C., van Lint, H., 2011. Anisotropy in generic multi-class traffic flow models. Transportmetrica 1.

Weidmann, U., 1993. Transporttechnik der Fussgänger. Schriftenreihe des IVT 90. Institut für Verkehrsplanung.

Xiong, M., Lees, M., Cai, W., Zhou, S., Low, M., 2010. Hybrid modelling of crowd simulation, in: International Conference on Computational Science, ICCS 2010, Procedia Computer Science. pp. 57–65.

Xiong, M., Tang, S., Zhao, D., 2013. A hybrid model for simulating crowd evacuation. New Generation Computing 13, 211–235.